

Electronic Supplementary Material (ESI) for RSC Advances.  
This journal is © The Royal Society of Chemistry 2017

## Electronic Supplementary Information

# **Magnetic porous graphene/multi-walled carbon nanotube beads from microfluidics: a flexible and robust oil/water separation material**

Zhipeng Bu,<sup>a, b, c</sup> Linlin Zang,<sup>d</sup> Yanhong Zhang,<sup>\*b</sup> Xiaojian Cao,<sup>a, b</sup> Liguao Sun,<sup>\*c</sup> Chuanli Qin<sup>a, b</sup> and Cheng Wang<sup>\*a</sup>

<sup>a</sup> Key Laboratory of Functional Inorganic Material Chemistry (MOE), Heilongjiang University, Harbin, 150080, China. E-mail address: wangc\_93@163.com

<sup>b</sup> School of Chemical Engineering and Materials, Heilongjiang University, Harbin, 150080, China. E-mail address: zhangyanhong1996@163.com

<sup>c</sup> Key Laboratory of Chemical Engineering Process & Technology for High-efficiency Conversion, College of Heilongjiang Province, School of Chemical Engineering and Materials, Heilongjiang University, Harbin, 150080, China. E-mail address: sunliguo1975@163.com

<sup>d</sup> State Key Laboratory of Urban Water Resource and Environment, Harbin Institute of Technology, Harbin, 150080, China

## **Preparation**

### **The synthesis of polystyrene (PS) microspheres.**

In a typical experiment to prepare PS microspheres with particle size of 283 nm, styrene (50 mL), methyl methacrylate (12 mL) and deionized water (500 mL) were added into a three necked flask under high-speed stirring of 300 rpm at 80 °C. After boiled for 5 min, potassium persulfate (0.5 g) was added to the mixed solution and kept stably refluxing for 2 h, followed by repeatedly centrifuged and dried at 60 °C. Finally, the solid products were obtained for further use.

### **The preparation of Fe<sub>3</sub>O<sub>4</sub> nanoparticles.**

Typically, anhydrous FeCl<sub>3</sub> (4 mmol) was added to diethylene glycol (50 mL) under vigorous stirring for 50 min. Sodium citrate (1.6 mmol) was added slowly and the solution was heated to 80 °C for 30 min. Following this, sodium acetate (12 mmol) was added until the mixture was

homogeneous. Next, the resultant solution was transferred to the Teflon-lined autoclave and maintained it at 240 °C for 6 h. After natural cooled to room temperature, the obtained black solution was centrifuged at 10000 rpm for 30 min and washed with ethyl alcohol for three times to remove the impurities. Finally, the products were obtained after dried at 60 °C for further use.

## Characterization

In order to study the effect of graphene on its structures and properties, additional four kinds of MPGCBs with different mass ratios of GO and aMWCNTs (10:0, 7:3, 5:5 and 0:10) were successfully fabricated. It can be clearly seen in Fig. 2d and S7 that the interconnected porous structure created by the removal of PS microspheres hard templates was formed in the all MPGCBs. It was worth noting that when the mass ratios of GO to aMWCNTs was at 5:5 and 0:10, honeycomb-like macropores were not richer than the other MPGCBs prepared with other three mass ratios (10:0, 7:3 and 3:7). This is because that the appropriate amount of graphene connected with MWCNTs could enhance the stability of skeleton structure. Even so, we consider that the abundant macropores in the MPGCBs will be beneficial for their absorption and separation in water treatment.

When used as oil/water separation material, robust mechanical property is critical for their use in harsh conditions. In a typical experiment, two detection modes containing compression and shear flow test were carried out (Fig. 4). The results indicated that the MPGCBs (3:7) possessed excellent mechanical property. In order to clarify the relations between the strength and mass ratios, shore hardness test was performed (Fig. S8). It was not difficult to find that the graphene combined with MWCNTs enhanced the hardness of the MPGCBs, which was owing to the synergistic effect between them in the scaffold. In addition, when the mass ratio of GO and aMWCNTs was at 3:7, the tested shore hardness reached to be maximized. This is because that the  $\pi$ - $\pi$  stacking interaction between graphene and MWCNTs play the role in entanglement to the utmost degree, and finally leading to the stability of spherical structure. These results demonstrated that the MPGCBs were probably suitable for water treatment in harsh conditions.

The MPGCBs with interconnected porous structure made it a potential candidate for the removal of oils and organic solvents from water. In a typical experiment, pump oil and chloroform were utilized to study the absorption behavior of MPGCBs fabricated with different mass ratios of

GO and aMWCNTs. As shown in Fig. S10, the MPGCBs possessed a high absorption capacity of 14 times its own weight for pump oil and chloroform. As expected, the MPGCBs (3:7) had the highest absorption capacity due to the stability of the constructed skeleton structure. And there is no definite effect of graphene on its absorption property. In general, the MPGCBs (3:7) should be the most suitable absorbent for oil/water separation.

Herein, S-1 (water-in-toluene) emulsion was used to evaluate the separation capacity of the MPGCBs prepared with different ratios of GO and aMWCNTs. It can be seen in Fig. S15 (black line) that the flux of the all MPGCBs is more than  $300 \text{ L/m}^2 \text{ h}^{-1} \text{ bar}^{-1}$ . By changing the mass ratios of GO and aMWCNTs, the MPGCBs (3:7) exhibit a promising flux of  $\sim 400 \text{ L/m}^2 \text{ h}^{-1} \text{ bar}^{-1}$ , which is significantly higher than that of the other MPGCBs. To further evaluate the separation efficiency, the oil purity in the corresponding filtrate was tested by a moisture titrator. As shown in Fig. S15 (blue line), the oil purity of the all filtrate can be up to 99.90 %, which indicated the excellent separation efficiency for all of the MPGCBs.

Therefore, the MPGCBs (3:7) possessed not only the most abundant and stable interconnected macroporous structure, but also had the highest mechanical property and separation capacity, which was of benefit to use as separation material in real water treatment.

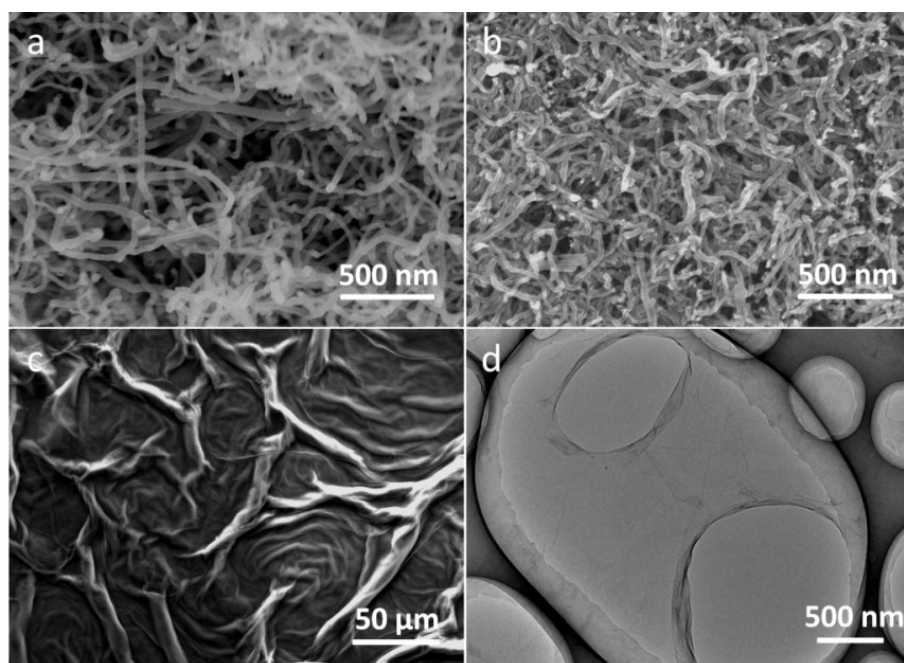


**Fig. S1** (a) and (b) were SEM images of MWCNTs and aMWCNTs, respectively. (c) and (d) were SEM image and TEM image of GO, respectively.

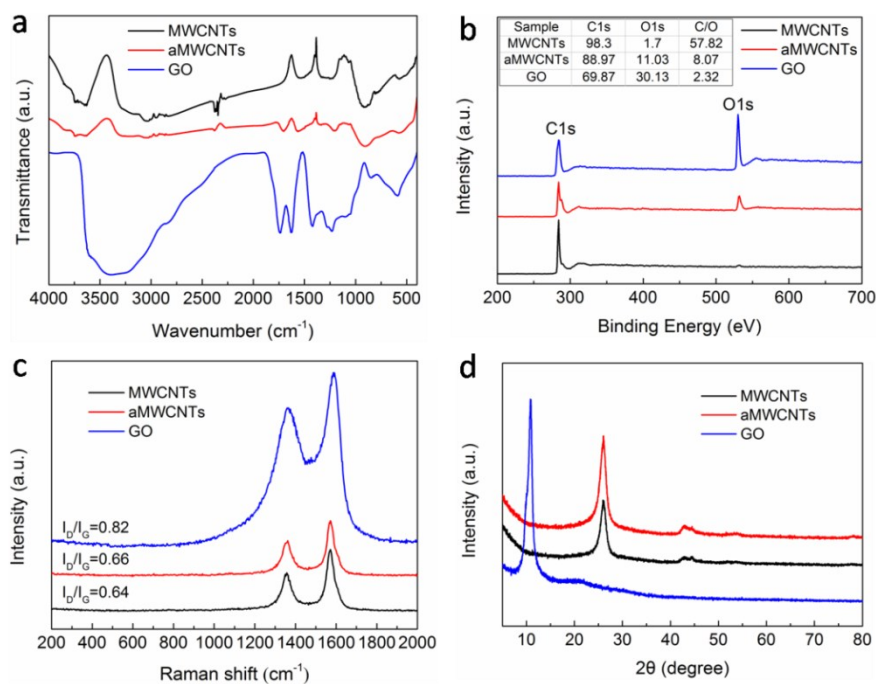


**Fig. S2** (a) FTIR spectra, (b) XPS spectra, (c) Raman spectra, and (d) XRD patterns of MWCNTs, aMWCNTs and GO.

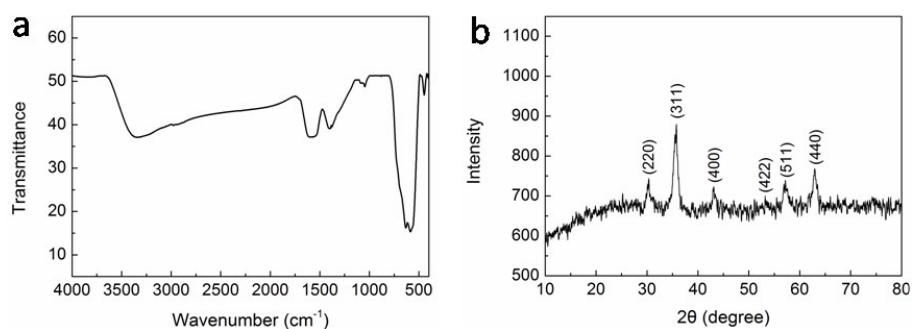


**Fig. S3** FTIR spectra (a) and (b) XRD pattern of  $\text{Fe}_3\text{O}_4$  nanoparticles.

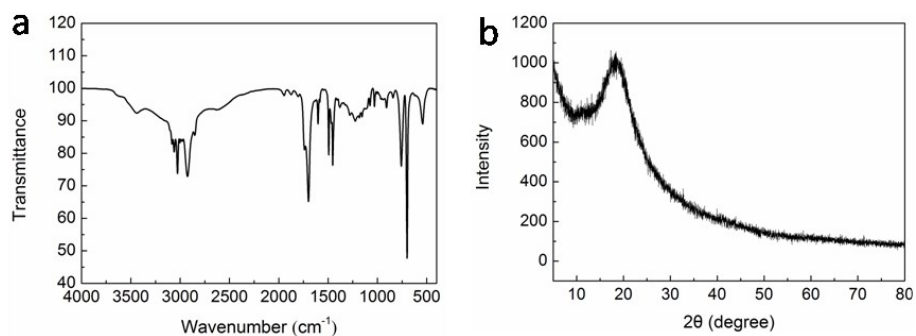


**Fig. S4** FTIR spectra (a) and (b) XRD pattern of PS microspheres.

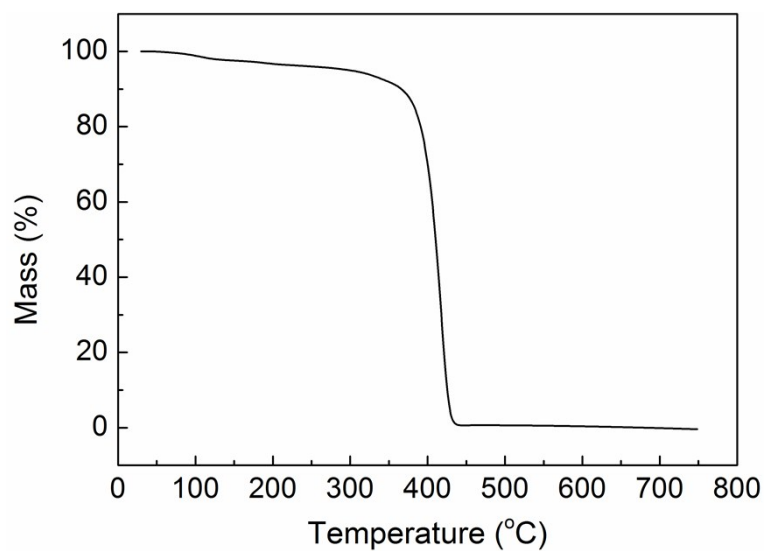


**Fig. S5** TGA curve of the PS microspheres that were performed under N<sub>2</sub> atmosphere and a heating rate of 5 °C • min<sup>-1</sup> from 30 to 750 °C.

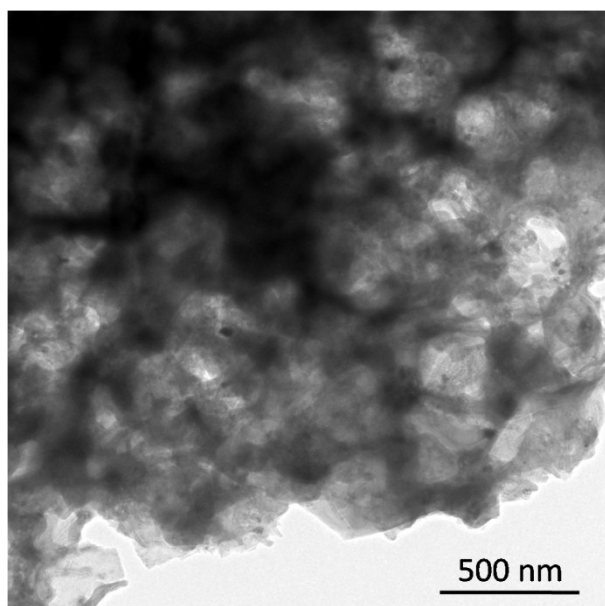


**Fig. S6** TEM image of the internal structure of the MPGCBs with mass ratio of 3:7.

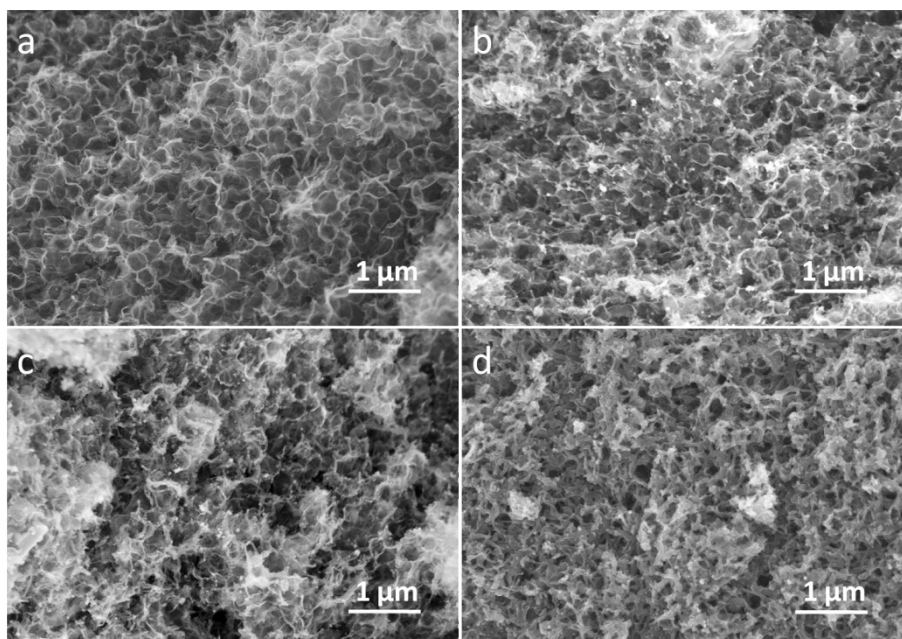


**Fig. S7** SEM images of the internal structure of MPGCBs with different mass ratios of GO and aMWCNTs: (a) 10:0, (b) 7:3, (c) 5:5 and (d) 0:10.

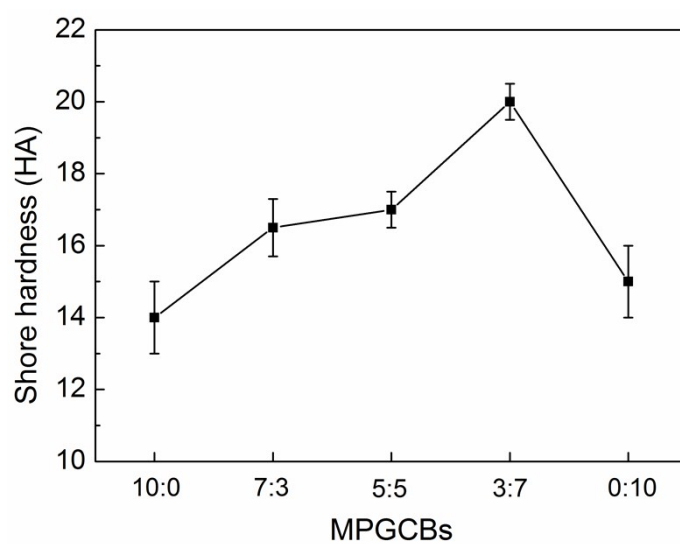


**Fig. S8** Shore hardness of MPGCBs with different mass ratios of GO and aMWCNTs.

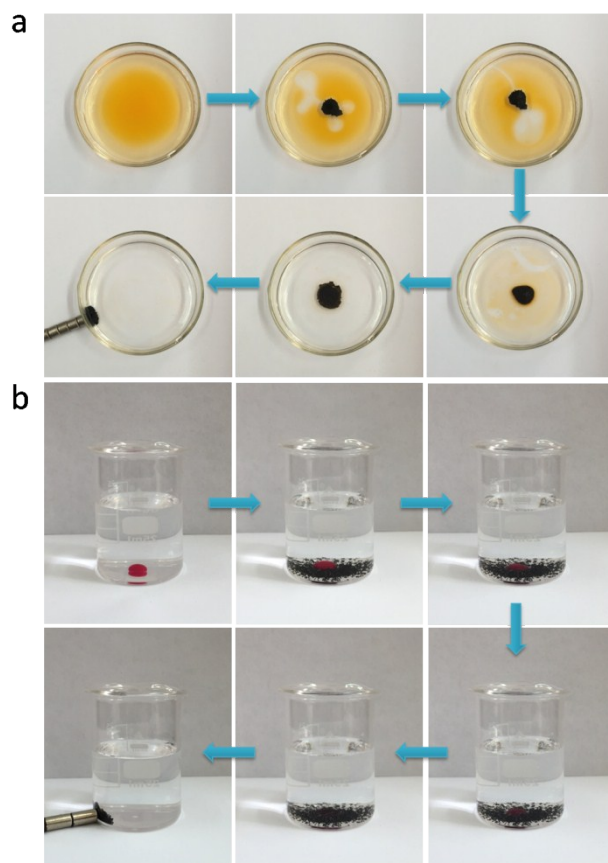


**Fig. S9** Digital photographs of absorption process using MPGCBs: (a) pump oil (orange) floating on the water surface and (b) chloroform (dark pink) under the water.

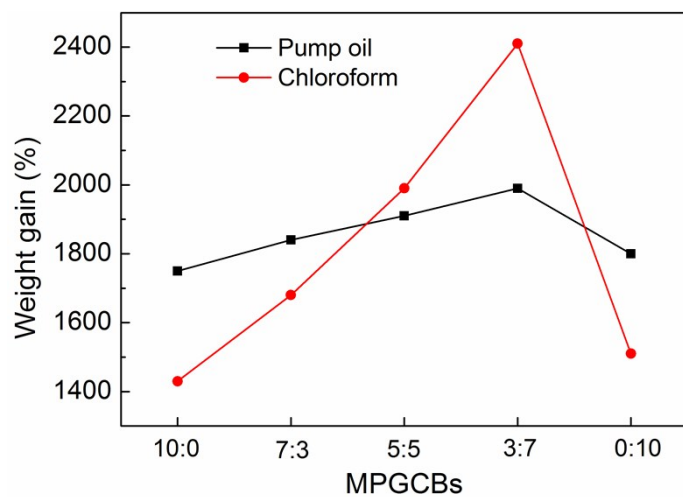


**Fig. S10** Absorption capacity of MPGCBs with different mass ratios of GO and aMWCNTs (10:0, 7:3, 5:5, 3:7 and 0:10) for pump oil and chloroform.

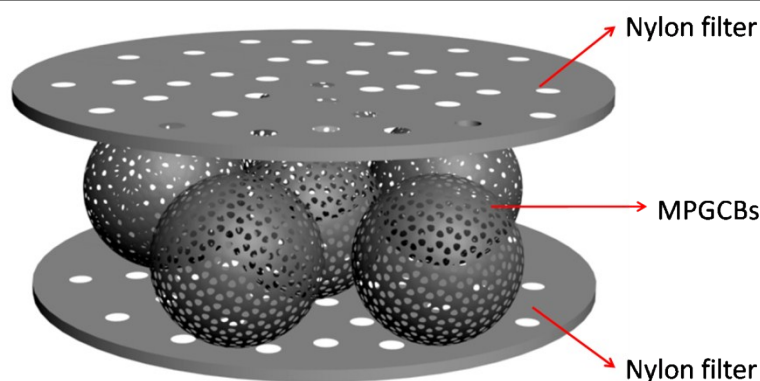
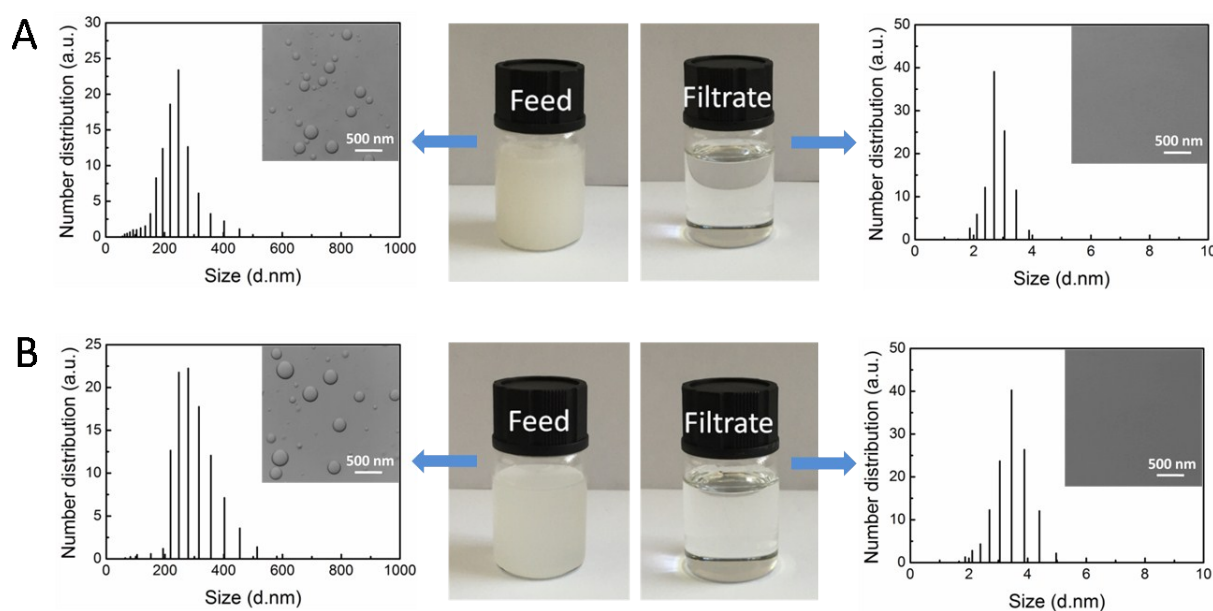


**Table S1** The composition and the droplet size of various emulsions.

Emulsion label	Oil	Water	Span-80	Droplet size	
S-1	Toluene	150 mL	1 mL	0.8 g	60~400 nm
S-2	Chloroform	150 mL	1 mL	1.2 g	50~500 nm
S-3	Hexane	150 mL	1 mL	1 g	40~600 nm

**Table S2** Viscosity, refractive index and density of the oils used in oil/water separation experiment.

Oil	Viscosity (mPa·s, 20 °C)	Refractive index ( $n_D^{20}$ )	Density (g/cm <sup>3</sup> )
Toluene	0.587	1.498	0.866
Chloroform	0.563	1.442	1.498
Hexane	0.307	1.378	0.659

**Fig. S11** Schematic diagram of the preparation of the sandwich-like filtration membrane.**Fig. S12** Photographs, optical microscopy images and DLS data of the feed and the corresponding filtrate for S-2 emulsion (A) and S-3 emulsion (B).



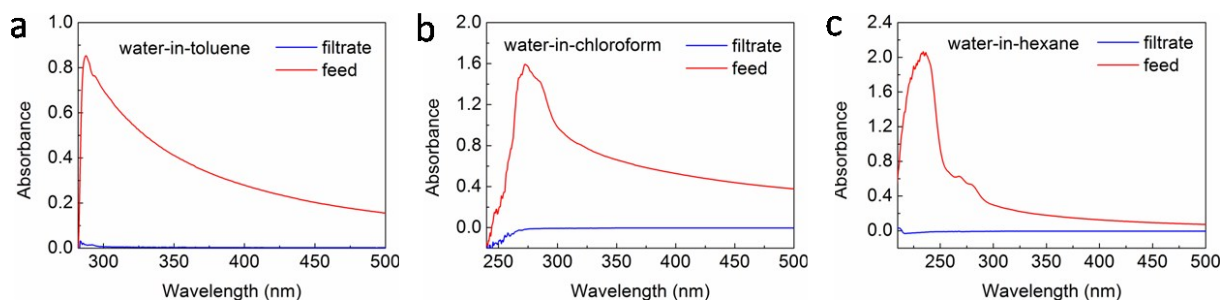


**Fig. S13** UV-vis spectra of S-1 (a), S-2 (b) and S-3 (c) emulsions before and after filtration.

### Calculation of the fluxes of MPGCBs.

The flux of MPGCBs was calculated using the following formula:

$$Flux = V / S t$$

The flux of MPGCBs depends on the penetrated volume in unit time. For this equation, V is the volume of the penetrated emulsion, S is the valid contact area of the fixed MPGCBs and t is the separating time.

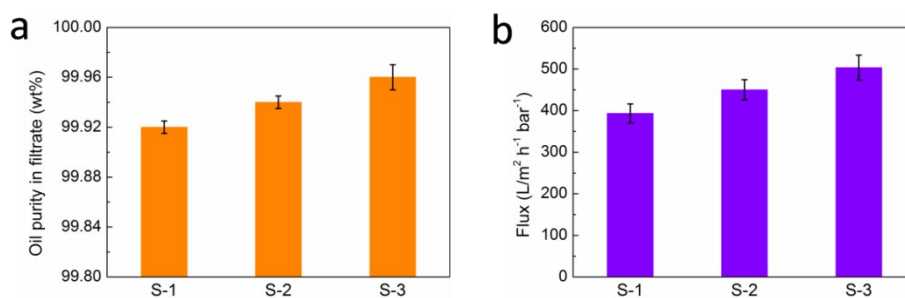


**Fig. S14** (a) Oil purity in the filtrate after S-1, S-2 and S-3 emulsions selective passed through the vacuum-driven filtration cell at 0.09 MPa, (b) Flux data of S-1, S-2 and S-3 emulsions passing through the vacuum-driven filtration cell at 0.09 MPa.

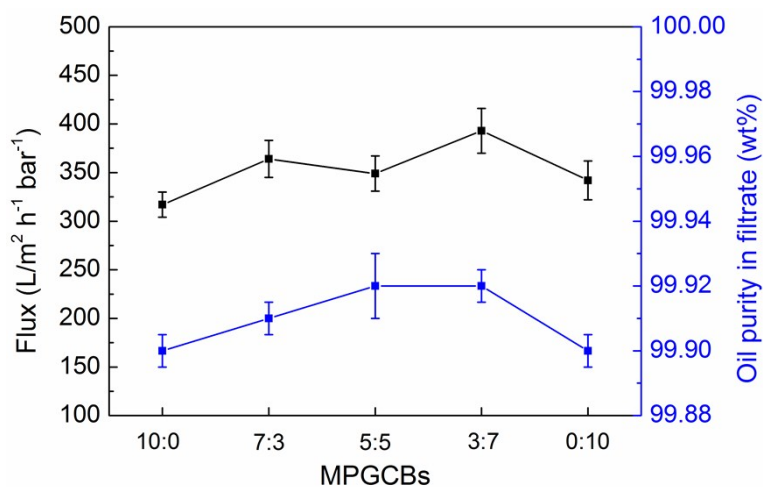


**Fig. S15** Flux data and oil purity in filtrate after S-1 emulsions selective passed through the vacuum-driven filtration cell at 0.09 MPa. The MPGCBs used in filtration cell were prepared by

adding different mass ratios of GO and aMWCNTs (10:0, 7:3, 5:5, 3:7 and 0:10).

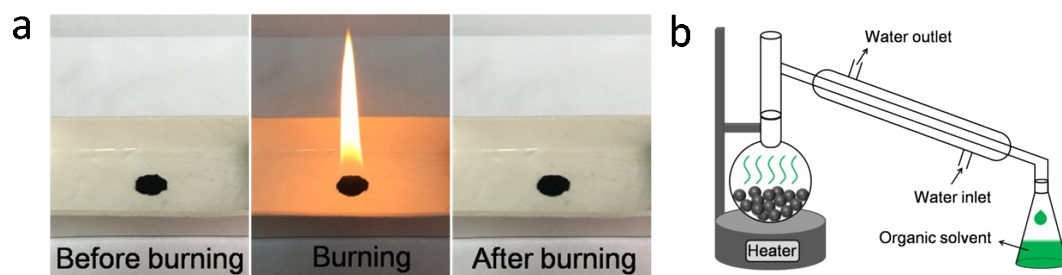


**Fig. S16** (a) Photographs showing the progress of recycling MPGCBs via combustion, (b) diagram showing the progress of recycling MPGCBs via distillation.